

Recoil of a liquid filament: escape from pinch-off through creation of a vortex ring

Jérôme Hoepffner[†] and Gounséti Paré

UPMC Univ Paris 06 & CNRS, UMR 7190, Institut Jean Le Rond d'Alembert, F-75005 Paris,
France.

(Received 10 July 2013)

A liquid filament recoils because of its surface tension. It may recoil to one sphere: the geometrical shape with lowest surface, or otherwise segment to several pieces which individually will recoil to spheres. This experiment is classical and its exploration is fundamental to the understanding of how liquid volumes relax. In this paper, we uncover a mechanism involving the creation of a vortex ring which plays a central role in escaping segmentation. The retracting blob is connected to the untouched filament by a neck. The radius of the neck decreases in time such that we may expect pinch-off. There is a flow through the neck because of the retraction. This flow may detach into a jet downstream of the neck when fluid viscosity exceeds a threshold. This sudden detachment creates a vortex ring which strongly modifies the flow pressure: fluid is expelled back into the neck which in turn reopens.

1. Introduction

A body of liquid with a given shape evolves because of its surface tension. Surface tension acts such as to reduce the total surface. One may think that this effect will lead any liquid volume to relax to the spherical shape, because the sphere is the shape for a given volume which has smallest area. But it is not always so: relaxation may lead to segmentation into several spheres. Why is it so? Because surface tension acts quickly, and it may be faster to reduce surface by cutting than by regrouping. Reducing area locally rather than globally may require to move less mass.

The Rayleigh-Plateau instability is the archetype for making drops out of a body of liquid, see Plateau (1873); Rayleigh (1879). Consider an infinite cylinder of liquid at rest; the perfect cylinder is a steady state which is unstable: when its surface is perturbed with a periodic wave of wavelength larger than its perimeter, the amplitude of the wave is led to grow in time to the eventual creation of a periodic train of drops. The ultimate process of segmentation is in itself very complex. To look at it, we may zoom at the location where the neck is thinnest, this is the region of a singularity: the neck shrinks at a dramatically increasing rate, down to a singularity in finite time with local self-similar behaviour, see for instance Eggers & Dupont (1994).

On the other hand, most cylinders are finite. Stone *et al.* (1986); Stone & Leal (1989) showed that we are in the need for yet another archetype to encompass the creation of drops at the retracting tip; an archetype which they coined *end-pinching*. Consider a filament of finite half-length L . Far from the two tips, the cylinder is locally at steady state, but at the tip, the pressure increase due to the curvature can only be balanced by the inertia of the retracting blob. If the filament is reasonably clean, the processes

[†] Email address for correspondence: jerome.hoepffner@upmc.fr

2

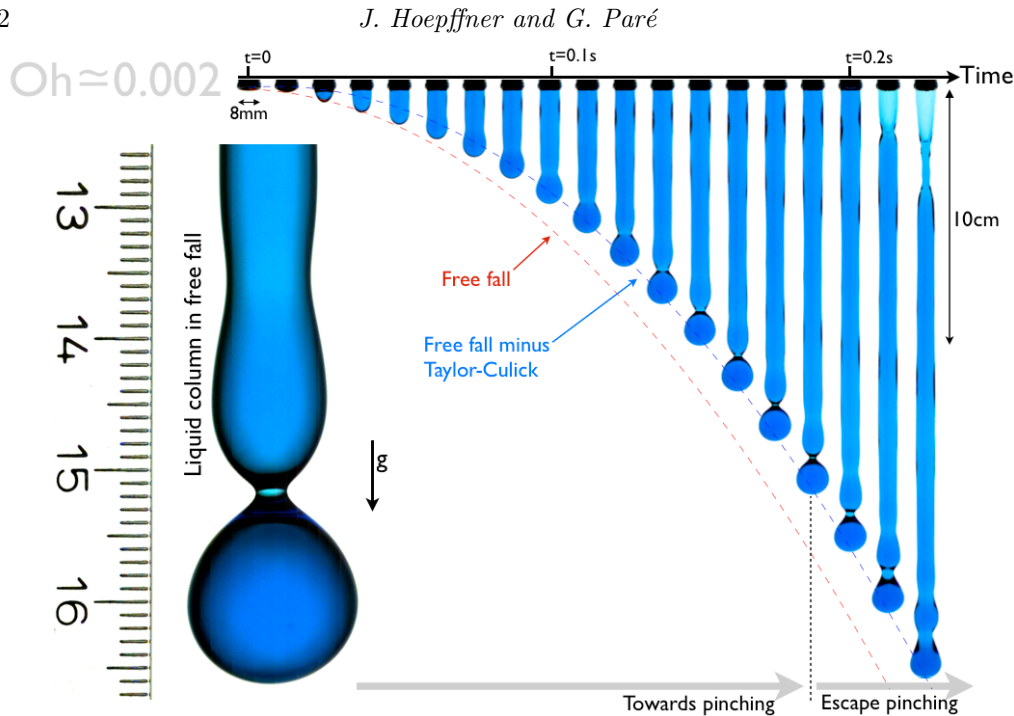


FIGURE 1. Display of the phenomenon of *escape*. A column of liquid is let free from a vertical straw. Its tip recoils and builds a neck which shrinks at first towards end-pinching. Unexpectedly, the neck reopens and a new capillary wave is sent upon the liquid cylinder. See movie I in the supplementary material for a video of this experiment.

linked to the retraction of the tip will dominate the Rayleigh-Plateau instability along the filament: drops are created preferentially from the segmentation of the retracting blob. It is on the tips that we must focus if we are to understand whether the filament relaxes to one sphere or to several spheres.

The tip retracts under the natural tension of the surface. Keller & Miksis (1983) is an inspiring article discussing capillary retraction. They showed that an inviscid liquid wedge retracts as a self-similar capillary wave. Indeed, dimensional analysis confirms that there is only one natural length scale, which can be built upon the growing time: $L = (\sigma t^2 / \rho)^{1/3}$, with σ the surface tension, ρ the fluid density, and t the time. The exact shape of the capillary wave of retraction is a function of the wedge opening angle. The study was pursued by Sierou & Lister (2004) who considered the retraction of a cone of an inviscid liquid. The main difference between the 2D wedge and the axisymmetrical cone is that the cone may be subject to the Rayleigh-Plateau instability. For the cone, the retraction is as well self-similar, and the most intriguing consequence of this self-similarity is that the tip does not pinch: the only cone that may pinch is that with zero opening angle. This is a subtle consequence of the dimensionality of this problem: the necks may shrink just at the same rate as the global capillary retraction along the cone of increasing cross-section.

The situation is different for a retracting filament: the section does not increase to compensate for the tendency to segment. The liquid at the retracting tip is collected inside a blob of growing size. A natural observable is the speed at which this retraction happens. See Taylor (1959); Culick (1960) for a planar sheet and Keller (1983); Keller *et al.* (1995) for a cylindrical filament. The momentum balance over a domain surrounding the blob

tells that the pull of the surface tension and the push of the cylinder inner pressure at the neck must be compensated for by the increase of momentum inside the blob. This yields the constant speed $u_{cap} = \sqrt{\sigma/\rho R}$, this is the *Taylor-Culick speed*. This formula is valid for the retraction velocity reached after the initial transient of acceleration. Note that the formula in Keller (1983) is overestimated by a factor of $\sqrt{2}$ because the cylinder inner pressure σ/R was not accounted for.

Far from the blob, the cylinder is stationary, it is locally at a steady state: the surface tension on the curved interface is locally counteracted by an increased inner pressure, this is the Laplace pressure jump, $\Delta p = \sigma/R$, with σ the surface tension and R the filament radius. See Laplace (1805) for the historical reference and De Gennes *et al.* (2004) for a recent book. We must now discuss the details of the anatomy of this blob. For short times, the region where the blob is connected to the cylinder shows locally an increase of diameter. See figure 6 below for a sketch. This means that in the region connecting the cylinder to the blob there are two components of surface curvature: that related to the cylinder radius, and as well a curvature along the axis of the cylinder. The tension associated with this latter curvature has the opposite effect of reducing the inside pressure: the centre of curvature is outside of the liquid, so the surface tension is pulling out. This must be balanced by a decrease of the inside pressure. Thus, the pressure just at the entrance of the blob is lower than that inside the cylinder. This pressure gradient induces a back flux: fluid from the cylinder gets sucked towards the blob while the blob retracts to swallow the cylinder. This back flow creates a neck. This phenomenon is described in Stone & Leal (1989) for viscous fluids. Once the neck is created, the associated new surface curvatures will be responsible for pressure jumps across the interface, thus a new evolution is started. This neck is a dedicated site for the Rayleigh-Plateau instability, we observe that the neck starts to reduce in diameter—shrinks—possibly towards *end-pinching*.

In the routine of our daily investigations, we came upon a peculiar observation. While inspecting a numerical simulation of a recoiling filament, just at the time when we would have expected the pinch-off, we observed instead a sudden reopening of the neck: the filament had escaped a dramatic fate, and a new capillary wave was created. Subsequent dedicated experiments showed that this event was always coincident with the creation of a vortex ring from the neck into the blob.

We found a similar observation in Notz & Basaran (2004). The 1D model of Eggers & Dupont (1994) is today a common tool to study the evolution of liquid filaments. This model extracted from the Navier–Stokes equations describes the evolving radius, pressure and axial velocity along the filament axis. It is widely used, see Eggers (1997); Eggers & Villermaux (2008); Brenner *et al.* (1997) and was for instance the key tool to the description of the self-similar pinch-off of the dripping faucet. Notz & Basaran (2004) showed that this 1D model unexpectedly could not reproduce the retraction of a filament of intermediate viscosity. It predicts pinch-off much too early. They showed using simulations of the Navier-Stokes equations that indeed a thin region of vorticity was generated downstream of the neck, an effect difficult to model in 1D. Unfortunately, Notz & Basaran (2004) did not see the creation of the vortex ring and could not analyse the decisive process actually responsible for the escape. Nevertheless, Notz & Basaran (2004) understood that this phenomenon was linked to the delaying of the pinch-off. We find similar observations in Schulkes (1996). In the case of the retraction of a liquid sheet, Gordillo *et al.* (2011) report the detachment of the jet from the neck to the blob; on the other hand in 2D, there is no instability actively leading to pinch-off so this event has less impact.

In the present paper, we are interested in understanding the mechanisms that lead to

pinch-off or escape: recoil to a sphere, or segment then recoil to several spheres. Instead of considering like Stone *et al.* (1986); Stone & Leal (1989) a filament of a viscous fluid inside another viscous fluid, we consider like Schulkes (1996); Notz & Basaran (2004); Castrejón-Pita *et al.* (2012); Keller *et al.* (1995) a liquid filament surrounded by air. There are two parameters in the state diagram for this system: the filament initial aspect ratio: how slender is it? and the Ohnesorge number: how much is the retraction power of surface tension counteracted by inertia and viscosity? $Oh = \mu/\sqrt{\rho\sigma R}$ where μ is the fluid dynamic viscosity, and ρ is its density. For the sake of simplicity, we will call a filament "long" when it is slender and "viscous" when its Ohnesorge is large. The final purpose of the present paper is to reinterpret figure 5 of Castrejón-Pita *et al.* (2012), which gathers all the data from the literature on this problem, experimental and numerical.

2. Observations

Our experiment consists in letting fall a column of liquid initially contained inside a vertical straw. Figure 1 shows a representative sequence of this experiment. We see at the top of the photograph the bottom end of a 8mm diameter straw. When the straw is opened at its top, the column of liquid falls. Once free, its lower tip retracts, and we see the creation of the blob and the neck. The position of the tip of the filament is compared to the curve of free fall: the difference is the distance the filament has retracted.

The Ohnesorge for this particular experiment is $Oh \approx 0.002$ (the fluid is water mixed with blue food dye, with $\sigma \approx 72mJ/m^2$, $\rho \approx 999kg/m^3$, $\mu \approx 0.95mPa\cdot s$). We observe the creation of the blob and the neck. The neck shrinks progressively until a time shortly before 0.2s. It then reopens unexpectedly. This is the *escape* phenomenon. In this situation with water at 20 degrees Celsius, to give orders of magnitude of the Ohnesorge number, the filament diameter is respectively about 3cm, 0.3mm and $3\mu m$ for $Oh = 0.001, 0.01, 0.1$. To ensure that the air drag does not influence the dynamics of the filament, we can evaluate the value of the Weber number $\rho U^2 R/\sigma$. The liquid falls for about half a meter and reach thus a maximum velocity of about 3m/s. With a filament radius of 4mm, the Weber is about one half. At such a low Weber, rain drops for instance remain spherical.

Please note that the present situation differs significantly from that of water flowing from a tap. In our straw experiment, apart from a thin viscous boundary layer along the walls, the liquid column is wholly in free fall: there is no stretching. For the tap, on the other hand, since the flux is constant at the top, the acceleration of free falling particles induce stretching. See for instance Senchenko & Bohr (2005); Javadi *et al.* (2013) for the stability analysis of a viscous thread flowing out of a tap. For another stability analysis of a stretched filament see Marmottant & Villermaux (2004).

To investigate further this phenomenon, we run numerical simulations of a receding filament in a setting similar to that of Notz & Basaran (2004). We use the open source software *Gerris flow solver*, see Popinet (2009). The initial condition is half a cylindrical filament at rest with an hemispherical tip. Its radius is 1, surface tension 1, density 1, and viscosity μ , surrounded with an inviscid fluid of density 0.01; light enough to have little influence on the filament's dynamics. The initial length is 47.5, long enough to observe escape or pinching before reaching the domain of influence of the boundary conditions. The domain height is $L = 5$. The Navier–Stokes equations are discretised using the method of finite volumes in an axisymmetrical configuration. The software affords adaptive mesh refinement based on a mixed function of fluid vorticity and surface curvature. The smallest mesh size used is the height of the box divided by 2^9 . The simulation runs for about a day on a single processor of a standard desktop computer.

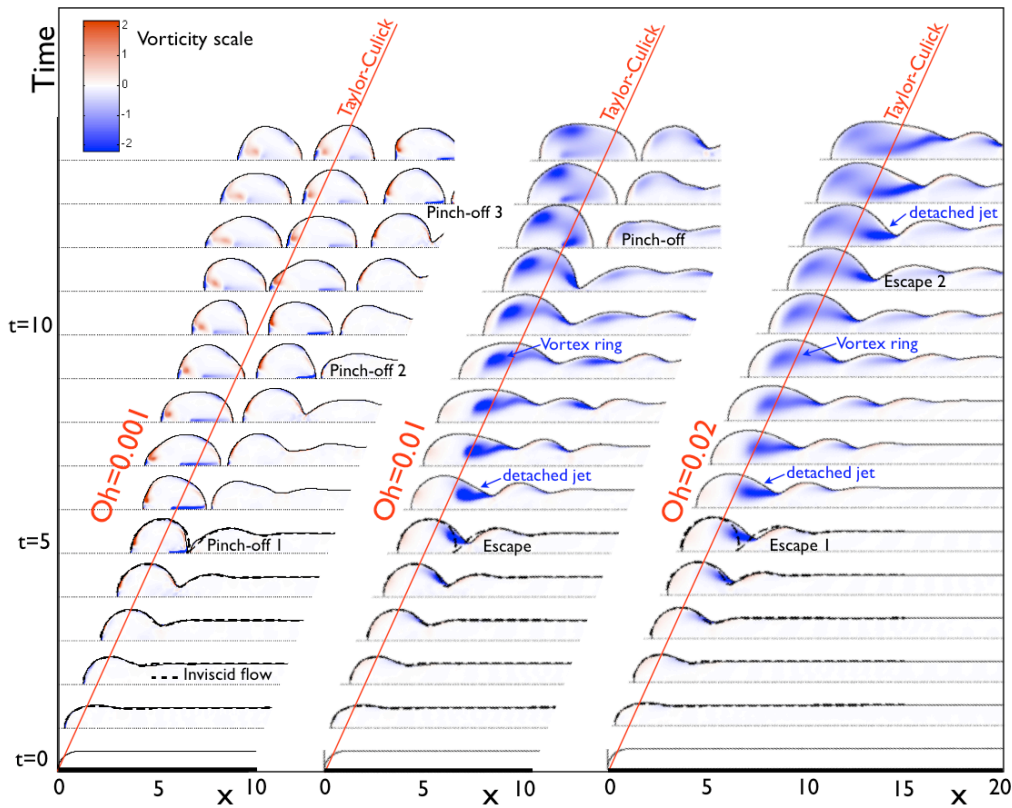


FIGURE 2. Numerical simulations of a recoiling filament for three values of the Ohnesorge number. Interface position and vorticity as a spatio-temporal diagram. Shown as a dashed line the inviscid flow evolution digitised from Schulkes (1996), obtained from a boundary integral numerical simulation. See movie V for the animation of the flow simulations.

The parameter file is available as a supplementary material to this paper. Gerris is free and easy to install on the Ubuntu Linux distribution. Using the parameter file, you can thus reproduce our numerical results without effort.

The results for three values of the Ohnesorge number are shown in figure 2. It displays a sequence of the interface position and the colormaps of the corresponding vorticity distributions. For $Oh = 0.001$ the evolution is very similar to the inviscid flow evolution digitised from Schulkes (1996) and shown as a dashed line. Pinch-off happens at time about 5 and a distance of about 7 from the initial tip location. For $Oh = 0.01$ the evolution is initially very similar, but instead of pinch-off, we observe the reopening of the neck and the formation of a vortex ring downstream of the neck (to its left). The filament then pinches-off later at time of about 11. For $Oh = 0.02$ we observe two successive escapes sequences.

We also show in the figure the Taylor-Culick retraction velocity as a guide to the eye. Note that we should not expect perfect match, since this velocity is designed to describe the retraction only at later times, once the blob is large compared to the filament's radius, after the initial transient which is shown here.

In figure 3 we show the evolution in time of the neck's radius for several values of the Ohnesorge number. For $Oh = 0.001$, the neck monotonously shrinks then pinches-off, in a manner very similar to the inviscid flow evolution. The case with $Oh = 0.01$ has

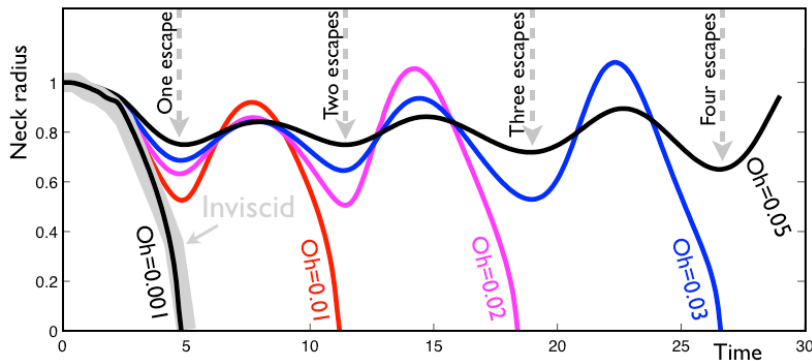


FIGURE 3. The radius of the neck evolving in time for several values of the Ohnesorge number (numerical simulations). When $Oh = 0.001$ the filament pinches directly, and so does the inviscid flow digitised from Schulkes (1996). For $Oh = 0.01$ we observe one escape then pinch, for $Oh = 0.02$ two escapes then pinch, and so on. See movie V of our supplementary material for a video of the numerical simulations.

one escape then pinch-off, $Oh = 0.02$ has two escapes then pinch-off. For $Oh = 0.05$, we observe four consecutive escapes. This can be also seen in the supplementary material on movie V for the numerical simulations. In that movie, you can see how each of these escape events is related to the creation of a vortex ring. We have also drawn the trajectories of tracer particles showing the jet at the neck and its detachment.

Figure 4 shows experimental observations of the vortical event. On the left a), we have mixed water with dark particles in order to trace the fluid particle trajectories. The filament is recorded as it falls in front of the camera. The images are then translated into the reference frame of the filament's tip. Successive images are superimposed according to minimal intensity with the open source software *ImageJ*. The vortex is clearly visible. Please note that the interface curvature distorts the image of the particles inside the filament, see for instance Gier & Wagner (2012), where particle image velocimetry is used to measure the velocity field inside a filament. See movie VI for the motion of tracer particles and movie II and III for the experiment with dye.

To visualise the vortex ring and the detached jet flow, we devise a procedure to assemble the liquid column as a stratified mixture of clear and dyed water. The results are shown in figure 4. The stratified situation is obtained as follows: we prepare half a litre of tap water mixed with 100 grams of table salt on one side, and half a litre of tap water mixed with blue food dye on the other side. The salt makes the clear water slightly heavier, this is useful to prevent mixing of the two fluids during the preparation of the experiment, such as to maintain a sharp dye front. The straw of 8mm inner diameter is first dipped in the coloured water until a desired depth $\ell = 6\text{cm}$, then the straw is closed at its top end and is dipped in the salty water down to depth ℓ again, such that the height of the surface inside and outside the straw coincide. Then the straw is opened at its top. Since the interface height is the same inside and outside, this situation is stationary. We then slowly dip the straw further down to depth $\ell + h$ with $h = 2.5\text{cm}$, close it again at the top. The straw is then closed at its top and withdrawn. In fact, instead of moving the straw with fixed containers, it is more practical to move the containers while the straw remains fixed. To reduce progressively the Ohnesorge number of the mixtures, we add the adequate quantity of ethanol into both containers (water $\sigma \approx 72\text{mJ/m}^2$, ethanol $\sigma \approx 22\text{mJ/m}^2$ at 20°C).

Figure 4b) shows the case of an Ohnesorge too small for escape. As the blob retracts,

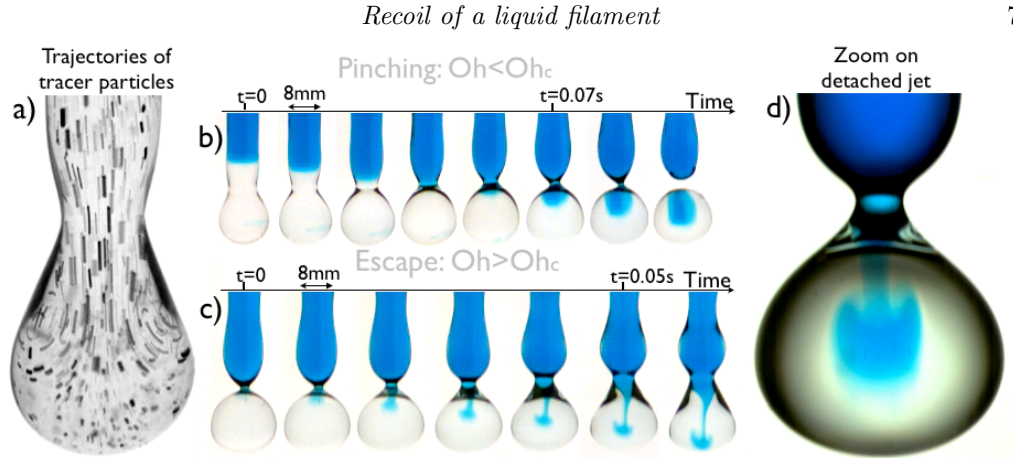


FIGURE 4. Experimental visualisation of the jet detachment. a) Particle trajectories after escape showing the vortex ring. The camera focus plane is thin to allow a sharp cut through the filament. b) For an Ohnesorge below criticality, visualisation of the dye front: no jet detachment. c) $Oh > Oh_c$ the jet detaches and we see the rolling-up of the tip of the dye jet due to the vortex ring. After reopening, the jet is reattached. d) Zoom on the jet. See movie II and III in our supplementary material.

the dye front moves towards the neck into the drop to be formed. The corresponding video is shown in movie II. Figure 4c) on the other hand shows a case with slightly larger Oh where the pinching is avoided. We chose the height h such that the creation of the vortex ring coincides with the arrival of the dye front at the neck. We can see that the Venturi is detached. We can as well see that the vortex ring is rolling up the tip of the dyed jet. Afterward, the neck reopens and the Venturi flow reattaches, which is readily visible because the dyed fluid has retaken the entire width of the expanding neck. We show on the right hand side of the figure an enlarged view of the filament with detached jet. This sequence of events is displayed in movie III.

With salt and ethanol, it is difficult to enforce the exact same value of the viscosity and surface tension for both fluids. For the escaping case of figure 4, the blue water has $Oh \approx 0.0048$ ($\sigma \approx 40mJ/m^2$, $\rho \approx 970kg/m^3$, $\mu \approx 4.8mPa s$) and the salty water has $Oh \approx 0.0058$ ($\sigma \approx 37mJ/m^2$, $\rho \approx 1068kg/m^3$, $\mu \approx 2.3mPa s$). The non-pinching case has a little less ethanol, thus a smaller Oh .

3. Analysis of the mechanism

To start with, we should try to find the simplest way to quantify the dynamics of the filament. For this we will start by following the linear stability analysis performed in Driessen *et al.* (2013), please see this reference for more details. Let us assume that the fate of the filament results from a competition between the time it takes for the Rayleigh-Plateau instability to segment the filament, and the time it takes for retraction of the blob. The cylindrical filament is subject to the Rayleigh-Plateau instability, that is, the evolution of the radius initially perturbed by a wave is

$$r(x, t) = R + \delta \exp(\omega t) \cos(kx/R)$$

where δ is the amplitude of the initial perturbation, $k = 2\pi/\lambda$ is the wavenumber and λ is the wavelength. Weber (1931) showed that the growth rate ω of the waves is

$$\omega_{cap} = \sqrt{(k^2 - k^4)/2 + 9/4 Oh^2 k^4 - 3/2 Oh k^2},$$

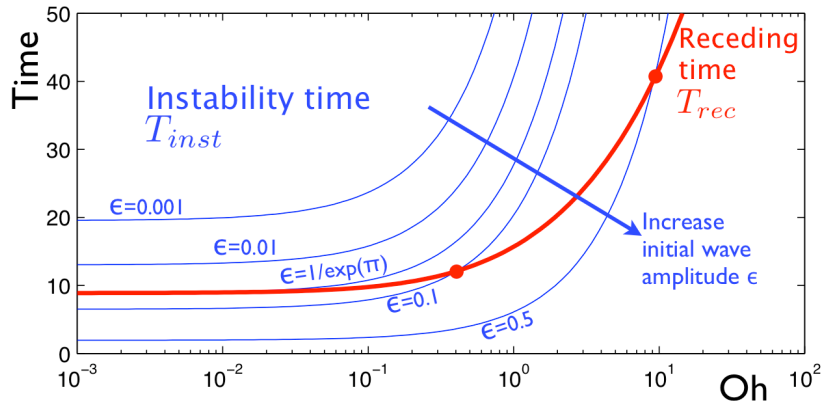


FIGURE 5. Comparison of the instability time T_{inst} and the retraction time over one wavelength T_{rec} from (3.1) and (3.2) as a function of the Ohnesorge number and for several values ϵ of the amplitude of the initial perturbation. Escape may happen whenever $T_{inst} < T_{rec}$.

with the capillary time $t_{cap} = \sqrt{\rho R^3/\sigma}$. The most unstable wavenumber is thus

$$k_{max} = 1/\sqrt{2 + 3\sqrt{2}Oh}.$$

Let us say that pinch-off is escaped whenever the time it takes for the capillary retraction over one wavelength of the most growing wave is less than the time it takes for segmentation by the instability wave. The segmentation time is the time it takes for the wave amplitude to reach R , that is

$$T_{inst} = \log(R/\delta)/\omega_{max} \quad (3.1)$$

where ω_{max} is the growth rate of the most unstable wave. The time it takes for capillary retraction over one wavelength is

$$T_{rec} = \lambda_{max}/\sqrt{\sigma/\rho R} \quad (3.2)$$

We compare these characteristic times in figure 5 for several values of the initial wave amplitude $\epsilon = \delta/R$. We see that for a low perturbation amplitude $\epsilon < 1/\exp(\pi) \sim 0.04$ the receding times wins over the instability time whatever the Ohnesorge: there is no time for the Rayleigh-Plateau instability to grow enough to yield pinch-off. For a large value of the initial perturbation amplitude on the other hand, there is a critical Ohnesorge below which the instability wins over retraction. For instance choosing $\epsilon = 0.1$, i.e. an initial wave of 10% of the filament's radius, for $Oh < 0.4$ the instability is fastest (pinch-off), and for $Oh > 0.4$ the retraction is fastest (escape).

This description has the right structure: for a moderate initial wave amplitude, it predicts pinch-off below a critical value of the Ohnesorge and escape above. On the other hand it is very sensitive on the initial amplitude ϵ of the perturbation: for low Ohnesorge, the curve of the instability time is nearly parallel to the curve of receding time. This is a problem because this initial wave amplitude is difficult to relate to the actual initiation of the retraction.

This description has the advantage that it is conceptually simple. On the other hand, it is not built upon the observations of the previous section, namely, the detachment of the jet downstream of the neck and the creation of a vortex ring. We move now to an alternative scenario of the mechanism of escape, akin to the spirit of *end-pinch-off* of Stone *et al.* (1986).

The mechanism is illustrated in figure 6. We already discussed the initial sequence of the tip retraction that leads to a blob and a neck (figure 6abc). We now discuss the subsequent evolution. Let us put ourselves in the reference frame moving with the neck (figure 6d). From there, we see the liquid from the filament flowing from the right at the Taylor-Culick receding velocity u_{cap} . Right at the neck, the radius of the filament is reduced, thus the flow from the filament into the blob must accelerate. Assuming a mostly inertial flow, the acceleration through the neck yields a decreased pressure.

The flow that we are describing is nothing else than the classical Venturi flow: the flow through a pipe with a local radius constriction. We know that this flow can be in two configuration: the *attached* configuration where downstream of the constriction, the fluid decelerates and recovers its high upstream pressure, or the *detached* configuration (see figure 6e) where the fast flow at the neck builds a jet with a recirculation region downstream of the constriction. This is the situation of a *head loss*: since the flow does not decelerate, it does not either recover its high upstream pressure.

There are two main differences between the classical Venturi flow and the flow induced by the retraction of the blob. First, our Venturi is not made with solid walls: the flow is constrained inside a fragile tensed interface who will deform in response to the variation of inner fluid pressure. We may call this flow a *capillary Venturi*. Second, this is not a stationary flow: there is initially a rapid acceleration towards the Taylor-Culick velocity and a progressive shrinking of the neck. The flow from the filament into the blob builds progressively a viscous boundary layer right at the constricted region. This special boundary layer is akin to that found around a rising bubble, see for instance Batchelor (1967). At the interface, the flow condition is not no-slip like in the Blasius boundary layer, but not-strain. The growth of this boundary layer is thus linked to the interface curvature, and happens only at the neck.

The neck shrinks on a capillary timescale $\sqrt{\rho R^3/\sigma}$ (see for instance the comparison between the inviscid flow evolution and our simulations in figure 2), whereas the boundary layer builds-up on a viscous time scale $\rho R^2/\mu$. The ratio of these two times is precisely the Ohnesorge number. Raising the Ohnesorge number imply that the viscous boundary layer grows faster, to such an extent that at $Oh \sim 0.0025$ it has grown enough to induce detachment of the Venturi jet before time $t = 5$ when capillarity segments the neck.

Why does the Venturi detachment prevent pinch-off? The jet detachment induces a sudden head-loss: the pressure downstream of the neck falls such that it can no longer counteract the squeezing effect of the capillary pressure of the surrounding interface. The fluid is squeezed away from this downstream region. It is expelled to the left into the blob and to the right back through the neck, which in turns reopens, as sketched in figure 6f.

Let us estimate the forces involved in this event: how long would it take to accelerate a fluid mass up to the retraction speed $\sqrt{\sigma/\rho R}$ from the pressure difference induced by the Venturi head loss? Assuming that the neck has a reduced radius R/n , then the jet velocity is n^2 times the retraction speed, thus the head is $\sigma/R(n^4 - 1)/2$. If this pressure drop is applied on a surface R^2 to accelerate a mass ρR^3 , then it takes $T = 2t_{cap}/(n^4 - 1)$ to reach the retraction velocity, with $t_{cap} = \sqrt{\rho R^3/\sigma}$ the capillary time. For instance for a halved radius at the neck ($n = 2$), it takes less than one capillary time to reopen the neck.

To check whether we can safely use the Bernoulli equations for the velocity/pressure relationship along the filament centreline, we may estimate the value of the Reynolds number at the neck. The Reynolds number based on the retraction velocity is $1/Oh$. We start to observe the escape event at about $Oh = 0.003$, which gives a Reynolds number based on the filament radius of about 300. With a neck of radius $R/2$ the local velocity

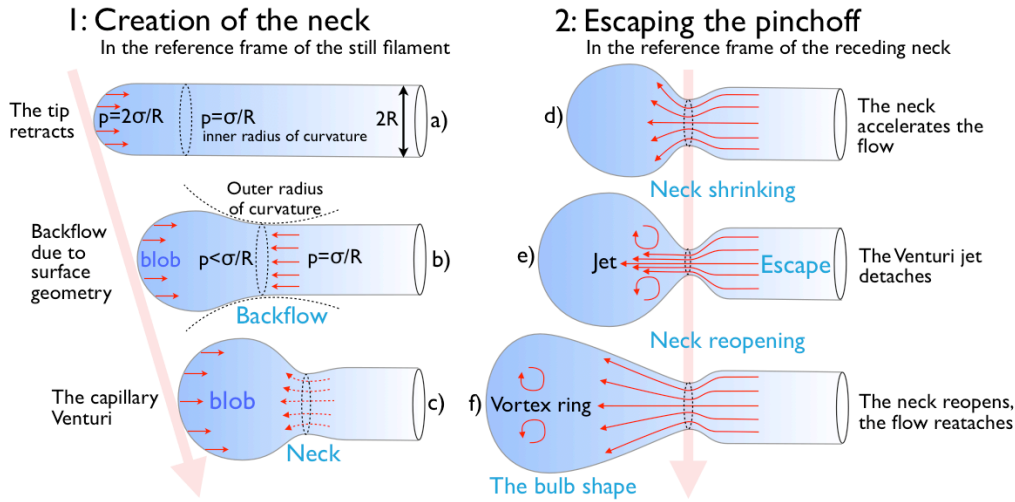


FIGURE 6. Description of the mechanisms active in the dynamics of the retracting tip of the filament. 1) Formation of the blob and the neck and 2) the detachment of the Venturi flow.

is four times the retraction velocity, thus at the neck we have $Re \approx 1200$ which is large enough to ensure the validity of the Bernoulli equation along the centreline streamline.

Of course this scenario is only a preliminary guess. We did not yet succeed in deriving a quantitative model that would confirm its fidelity to the actual phenomenon. We thought nevertheless that the reader might be interested in an explanation which includes the observed jet detachment.

4. Break-up of finite filaments

We have now described the phenomenon of escape in details, it is time to step back for a wider view on the recoiling filament. All numerical and experimental data available in the literature is summarised in figure 5 of Castrejón-Pita *et al.* (2012), see also our figure 7. Pinching and non-pinching filaments are identified in the filament aspect-ratio/Ohnesorge number plane. For a given Ohnesorge number, the data shows that below a critical filament length L_c , recoil yields a single sphere, whereas it segments for larger lengths. Furthermore, this critical length L_c increases with Ohnesorge: the more viscous, the longer the filament needs to be in order to pinch-off.

We would like to transpose the observations we have gathered here for a recoiling tip—a semi-infinite filament—to these published experimental results. To allow for this, we need to neglect what happens at the mid-length of the filament, where the two recoiling tips eventually meet; we assume that the break-up is neither significantly hindered nor encouraged at this region. The error bars of the data of Castrejón-Pita *et al.* (2012) and the difference between the experimental and numerical protocol secure this approximation. We refer to Notz & Basaran (2004); Castrejón-Pita *et al.* (2012); Schulkes (1996) for observations on the final dynamics. Here, we would rather like to bring to light the structure of the frontier between pinching and non-pinching filaments. We show that the escape is the hidden mechanism responsible for the increase of critical filament length L_c for viscous liquids.

The transposition we adopt to be able to do this comparison is the following: if a filament is initially shorter than the recoiling length it takes for a semi-infinite filament

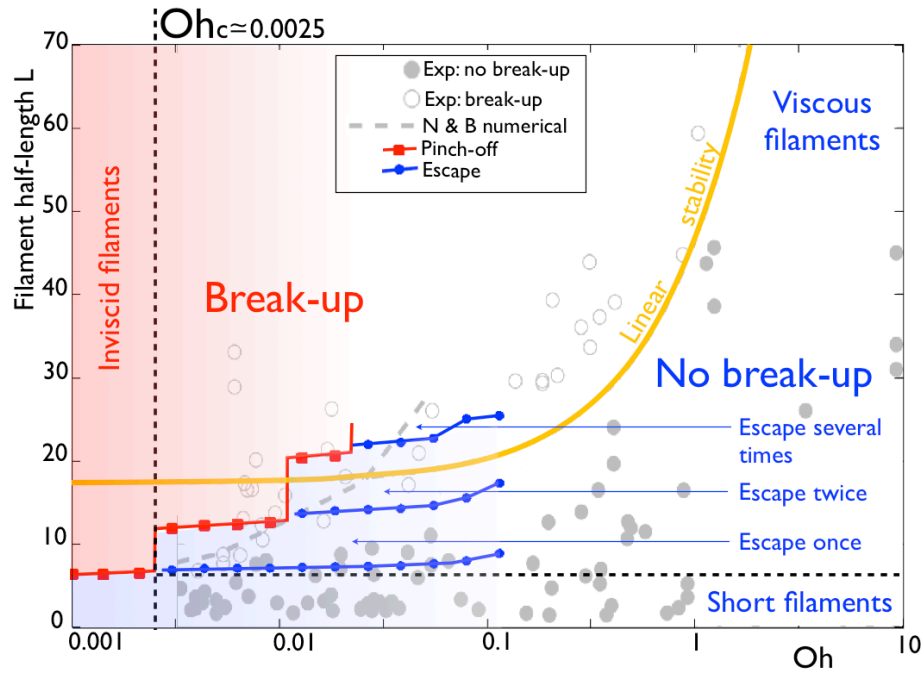


FIGURE 7. Fate of liquid filaments in the aspect ratio/Ohnesorge plane. Squares (red online) show the positions of pinch events, and dots (blue online) show the position of escape events from our numerical simulations. Experimental and numerical data from recoiling filaments are retrieved from Castrejón-Pita *et al.* (2012) and the figure is adapted from Driessen *et al.* (2013). The dashed light grey line is the numerical data from Notz & Basaran (2004), denoted in the legend as N&B. The light grey boundary (orange online) labelled "Linear stability" pertains to the Rayleigh-Plateau analysis of Driessen *et al.* (2013).

to pinch-off, then it does not pinch-off. If it has just the length it takes our filament to escape pinching once, then it recoils to a sphere after one single escape event. To draw this graph, we run numerical simulations for several Oh . An escape event is identified as the position which is a minimum of filament radius in space and time simultaneously; it is shown on the graph by a dot (blue online). A pinch-off event is localised as the position where the radius vanishes; it is denoted on the graph by a square (red online). From this data, we have drawn coloured zones corresponding to the filament's fate: grey (blue online) when it recoils to a single sphere, and light grey (red online) when it pinches-off to several spheres.

The results are displayed in figure 7. Notz & Basaran (2004) (Denoted N&B in the legend) have run simulations to find the frontier of L_c , it is displayed as a dashed line, this corresponds to their table 3. The frontier we predict with our simulations is in good agreement. We note on the other hand that our frontier has jumps. The first jump happens at $Oh \sim 0.002$, the second jump is at $Oh \sim 0.01$. Just above this Ohnesorge, we observe two consecutive escapes.

We decompose here the filament half-length/Ohnesorge plane in several identifiable regions: a region for $Oh > 1$ where the filament never pinches-off whatever its length, this is the *viscous filament regime*. A neck does not even appear in this regime. For $L_0 < 7$, the filament never pinches-off whatever its Ohnesorge, this is the *short filament regime*. We come now to the effect of the escape. We obtained that the largest Oh for which there is a direct pinch—no escape—is $0.0021 < Oh_c < 0.003$. We can thus identify the *inviscid*

filament regime for which viscosity is too low to allow build-up of shear regions and jet detachment. We have also represented the regions where there is one escape event, or several escape events. We observe for intermediate values of Oh as many as 3 consecutive escapes. With these values of viscosity, the escape is much less violent, with build-up of diffuse regions of vorticity in place of the clear shedding of a vortex ring. This is shown in movie V where we follow the evolution of interface and vorticity for several values of the Ohnesorge, and this is also seen in figure 3 for the evolution of the neck's radius.

The mechanism we describe here is most active at Ohnesorge number below 0.1. Driessen *et al.* (2013) on the other hand focused on the segmentation for long viscous filaments. They evaluate the possibility of segmentation from a growing Rayleigh–Plateau wave during the time it takes for complete capillary retraction. Viscosity does not affect the retraction velocity but slows down the linear instability, thus segmentation should happen for ever longer filament as viscosity is increased. We were inspired by their paper in §3 when comparing the time for capillary break-up to the receding time over one single wavelength of the most unstable wave. Doing this analysis by considering the receding time over the complete length of the filament yields a criterion for Rayleigh–Plateau fragmentation of the filament. This is drawn as the light grey boundary in figure 7 (orange online). Of course the position of this boundary depends on the initial perturbation amplitude just as it does in our analysis of §3, the value 0.01 for the wave initial amplitude yields a good fit of the experimental boundary for $Oh > 0.1$.

5. Conclusion

For Ohnesorge numbers below about 0.002, a liquid cylinder pinches along the mechanism of *end-pinchng*: the blob grows, builds a neck which segments. This neck resembles a capillary Venturi: it is a region of reduced radius moving along with the retracting blob. The fluid of the filament must be accelerated down the convergent and decelerated up the divergent before being gulped by the translating blob. Above this critical value of the Ohnesorge, the viscous boundary layer inside the capillary Venturi has time to grow to such an extent that the jet happens to detach. This detachment is the inception of a vortex ring inside the blob. This sudden event is violent and affects very much the pressure distribution inside the filament. The shape of the recoiling filament is a fragile balance of capillary pressure due to the surface curvature and the pressure related to the axial flow along the filament. Thus, this event will change the evolution and the shape of the filament. In particular, we observe that instead of pinching, the neck reopens: pinching is escaped. Unfortunately we do not have yet a quantitative model to confirm this interpretation. As ongoing work, we study the capillary Venturi in simpler configuration in order to get more insight into its dynamics.

This change in the dynamics of the system seeds a new capillary wave. The two capillary waves interact by addition and cancelation. After the escape, a new neck will be created from the interaction of these two waves of different origin. Pictures of the drops after complete segmentation of a liquid filament, like for instance in Marmottant & Villermaux (2004), show an apparently random distribution. We may here conjecture that this disorder results from the interference of the two capillary waves. The escape is thus responsible for avoiding segmentation of short filaments, but it may as well be taken as responsible for the apparent disorder of drop distribution after complete segmentation.

When a zone of contracted radius is in motion along a slender body of liquid, this region can be considered as a fragile Venturi. When the neck is too severe, a flow with moderate viscosity will build a zone of shear which may have time to detach before segmentation. If this phenomenon occurs, then the popular 1D set of equations used to model liquid

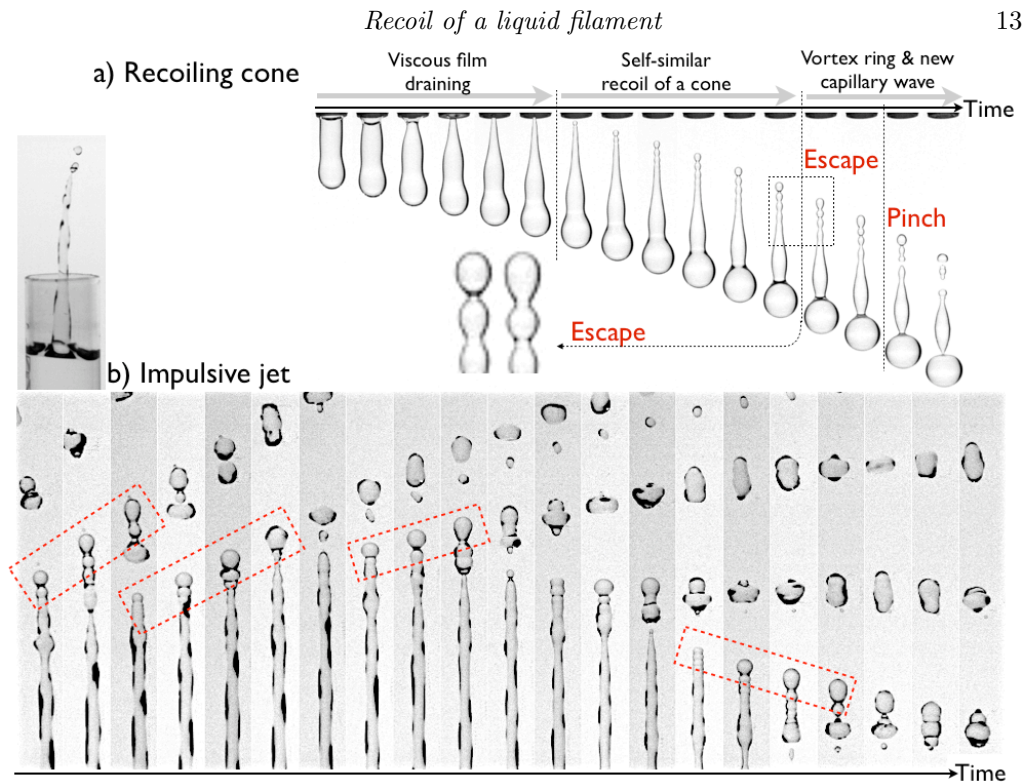


FIGURE 8. Generality of the escape event. a) A cone of water built from draining of the film along the straw walls. The cone recoils as a self-similar capillary wave and should not pinch, but we observe a sudden change of the blob, showing the bulb shape characteristic of the escape. b) Spatio-temporal diagram of a stretched water filament. The jet follows from impact of a falling test tube. Escape sequences are emphasised.

filaments, from Eggers & Dupont (1994) will fail to properly describe the evolution as shown in Notz & Basaran (2004). For these situations, it should be possible to add some more degrees of freedom in the 1D modelling to account for the flow separation, and thus be able to describe the escape using a related set of dynamic equations.

We may now wonder about the generality of the escape phenomenon: is this something very rarely observed, which will affect only the very situation described in our experiments? or is it something that can be found any time when a slender body of fluid is evolving? To answer this question we show in figure 8 two experiments that are easy to perform. The first one is the retraction of a liquid cone. This cone is obtained once the liquid column has fallen out of the straw, from the progressive draining of the liquid film which adheres by viscosity along the straw walls. As soon as the cone pinches from the straw, it starts to recoil. We observe on the figure the recoil capillary wave. As studied in Sierou & Lister (2004), this wave is self similar. But at some time, we recognise a sudden change in shape: the bulb—typical of post-escape blobs—appears. This event seeds a new capillary wave on top of the self-similar retraction wave. Subsequently, the cone pinches at several positions.

Another example is shown on the figure. Here we obtain a stretched liquid filament from the impact of a test tube following free fall as studied in Antkowiak *et al.* (2007). As discussed in Marmottant & Villermaux (2004), stretching stabilises the Rayleigh-Plateau instability, but drops are being created progressively from the rising tip. The stretching is

strong for the few first drops, there is then no flow through the neck. But this stretching decreases for the following drops. There must then be a competition between stretching from the initial impulse and capillary recoil. Several sequences which may be recognised as escapes are emphasised.

We are grateful to Arnaud Antkowiak, Howard Stone and Stéphane Zaleski for encouraging discussions. We thank José-Eduardo Weisfreid, Grégoire Lemoult and Sara Abdi for lending the tracer particles. We thank J. John Soundar Jerome for careful reading of the manuscript. We acknowledge financial support from the ANR VAA.

REFERENCES

- ANTKOWIAK, ARNAUD, BREMOND, NICOLAS & LE DIZÈS, STÉPHANE 2007 Short-term dynamics of a density interface following an impact. *J. Fluid Mech.* **577**, 241–250.
- BATCHELOR, G. K. 1967 *An introduction to fluid dynamics*. Cambridge university press, New York.
- BRENNER, MICHAEL, EGGERS, JENS, JOSEPH, KATHY, NAGEL, SIDNEY R. & SHI, X. D. 1997 Breakdown of scaling in droplet fission at high Reynolds number. *Phys. Fluids* **9**, 1573–1590.
- CASTREJÓN-PITA, ALFONSO A., CASTREJÓN-PITA, J. R. & HUTCHINGS, I. M. 2012 Breakup of liquid filaments. *Phys. Rev. Lett.* **108** (074506).
- CULICK, F. E. C. 1960 Comments on a ruptured soap film. *J. Appl. Phys.* **31**, 1128–1129.
- DE GENNES, PIERRE-GILLES, QUÉRÉ, DAVID & BROCHARD-WYART, FRANÇOISE 2004 *Capillary and wetting phenomena: Drops, bubble, pearls, waves*. Springer, New-York.
- DRIESSEN, THEO, JEURISSEN, ROGER, WIJSHOFF, HERMAN, TOSCHI, FEDERICO & LOHSE, DETLEF 2013 Stability of viscous long liquid filaments. *Submitted* .
- EGGERS, JENS 1997 Nonlinear dynamics and breakup of a free-surface flow. *Rev. Mod. Phys.* **69** (3), 865–929.
- EGGERS, JENS & DUPONT, TODD F. 1994 Drop formation in a one-dimensional approximation of the Navier-Stokes equation. *J. Fluid Mech.* **262**, 205–221.
- EGGERS, JENS & VILLERMAUX, EMMANUEL 2008 Physics of liquid jets. *Rep. Prog. Phys.* **71** (036601).
- GIER, S. & WAGNER, C. 2012 Visualization of the flow profile inside a thinning filament during capillary breakup of a polymer solution via particle image velocimetry and particle tracking velocimetry. *Phys. Fluids* **24** (053102).
- GORDILLO, LEONARDO, AGBAGLAH, GILOU, DUCHEMIN, LAURENT & JOSSEAND, CHRISTOPHE 2011 Asymptotic behaviour of a retracting two-dimensional fluid sheet. *Phys. Fluids* **23** (122101).
- JAVADI, A., EGGERS, J., BONN, D., HABIBI, M. & RIBE, N. M. 2013 Delayed capillary breakup of falling viscous jets. *Phys. Rev. Lett.* *Submitted* .
- KELLER, JOSEPH B. 1983 Breaking of liquid films and threads. *Phys. Fluids* **26**, 3451–3453.
- KELLER, JOSEPH B., KING, ANDREW & TING, LU 1995 Blob formation. *Phys. Fluids* **7**, 226–228.
- KELLER, JOSEPH B. & MIKSI, MICHAEL J. 1983 Surface tension driven flow. *SIAM J. App. Math.* **43** (2), 268–277.
- LAPLACE, PIERRE-SIMON 1805 *Traité de mécanique céleste*, , vol. Supplément au livre X. Courcier, Paris.
- MARMOTTANT, PHILIPPE & VILLERMAUX, EMMANUEL 2004 Fragmentation of stretched liquid ligaments. *Phys. Fluids* **16** (8), 2732–2741.
- NOTZ, PATRICK K. & BASARAN, OSMAN A. 2004 Dynamics and breakup of a contracting liquid filament. *J. Fluid Mech.* **512**, 223–256.
- PLATEAU, JOSEPH 1873 *Statique expérimentale et théorique des liquides soumis aux seules forces moléculaires*. Gauthier-Villars, Paris.
- POPINET, STÉPHANE 2009 An accurate adaptive solver for surface-tension-driven interfacial flows. *J. Comp. Phys.* **228**, 5838–5866.
- RAYLEIGH 1879 On the instability of jets. *Proc. Lond. Math. Soc.* **10**, 4–13.

- SCHULKES, R. M. S. M. 1996 The contraction of liquid filaments. *J. Fluid Mech.* **309**, 277–300.
- SENCHEENKO, SERGEY & BOHR, TOMAS 2005 Shape and stability of a viscous thread. *Physical review E* **71** (056301).
- SIEROU, ASIMINA & LISTER, JOHN R. 2004 Self-similar recoil of inviscid drops. *Phys. Fluids* **16** (5), 1379–1394.
- STONE, HOWARD A., BENTLEY, B. J. & LEAL, L. G. 1986 An experimental study of transient effects in the breakup of viscous drops. *J. Fluid Mech.* **173**, 131–158.
- STONE, HOWARD A. & LEAL, L. G. 1989 Relaxation and breakup of an initially extended drop in an otherwise quiescent fluid. *J. Fluid Mech.* **198**, 399–427.
- TAYLOR, G. I. 1959 The dynamics of thin sheets of fluids, III Disintegration of fluid sheets. *Proc. R. Soc. Lond. A.* **253** (313).
- WEBER, C. 1931 Zum Zerfall eines Flüssigkeitsstrahles. *ZAMM* **11**, 136.